



**HAL**  
open science

## Long-term solar heat storage process by absorption with the KCOOH/H<sub>2</sub>O couple: Experimental investigation

Nolwenn Le Pierrès, Fredy Huaylla, Benoit Stutz, Julien Perraud

### ► To cite this version:

Nolwenn Le Pierrès, Fredy Huaylla, Benoit Stutz, Julien Perraud. Long-term solar heat storage process by absorption with the KCOOH/H<sub>2</sub>O couple: Experimental investigation. *Energy*, 2017, 141, pp.1313-1323. 10.1016/j.energy.2017.10.111 . hal-01833447

**HAL Id: hal-01833447**

**<https://univ-smb.hal.science/hal-01833447v1>**

Submitted on 21 Nov 2018

**HAL** is a multi-disciplinary open access archive for the deposit and dissemination of scientific research documents, whether they are published or not. The documents may come from teaching and research institutions in France or abroad, or from public or private research centers.

L'archive ouverte pluridisciplinaire **HAL**, est destinée au dépôt et à la diffusion de documents scientifiques de niveau recherche, publiés ou non, émanant des établissements d'enseignement et de recherche français ou étrangers, des laboratoires publics ou privés.

# Long-term solar heat storage process by absorption with the KCOOH/H<sub>2</sub>O couple: Experimental investigation

LE PIERRES Nolwenn<sup>a\*</sup>, HUAYLLA Fredy<sup>a</sup>, STUTZ Benoit<sup>a</sup>, PERRAUD Julien<sup>a</sup>

<sup>a</sup>Laboratoire LOCIE, Université Savoie Mont Blanc-CNRS UMR5271

Savoie Technolac, 73376 Le Bourget-Du-Lac, France

## Abstract

This paper presents experimental results obtained with a prototype of a solar heat storage absorption process using the KCOOH/H<sub>2</sub>O couple. The process principle and the prototype tested are described, and both charging and discharging results are presented and discussed. The parameters influencing the results the most are water and solution flow on the reactor heat exchangers as well as the heat source and sink temperatures. The system's main limitation is the wetting of the exchanger plates. However, the tests prove the interest of the KCOOH/H<sub>2</sub>O couple in this type of low-temperature heat storage process.

**Keywords:** heat storage, KCOOH/H<sub>2</sub>O, absorption, solar heat, building

## 1. Introduction

About half of the world's final energy demand is used for heating and cooling purposes. The building sector consumes energy in large quantities, accounting for more than 30% of global final energy consumption (IEA, 2015). In this context, efficient and sustainable heat storage in buildings is one of the challenges to overcome in order to improve energy efficiency, take greater advantage of available renewable energies and avoid fossil fuel depletion and its environmental and social consequences. Sorption and thermochemical technologies present an advantageous option to store heat, both for high-temperature applications (Zhang et al., 2016; Wokon et al., 2017) and low-temperature space heating in buildings, because it allows storing heat over long periods, for example excess solar heat available during the summer until the following winter (N'Tsoukpoe et al., 2012). Sorption and thermochemical storage systems also have higher energy density compared to sensible and latent systems, as shown in Figure 1 (N'Tsoukpoe et al., 2009). Their operating conditions are compatible with the use of conventional solar heat collectors, thus contributing to more sustainable energies. Several research projects have been developed around this technology in recent years (Zhang et al., 2014; Ibrahim et al., 2017). However, until now no absorption system has reached the commercial stage, because of the difficulty finding an ideal absorption couple for this technology. Different interseasonal solar heat storage prototypes for heating purposes using gas/liquid sorption processes have been built and tested in the past. Among the low-temperature heat storage systems, all of them used water as sorbate. Four different sorbents have been tested: LiCl, CaCl<sub>2</sub>, NaOH and LiBr.

ClimateWell in Sweden (Bales and Nordlander, 2005) appears to be the leading pioneer in absorption heat storage systems. A sorption heat storage system based on a three-phase process (Yu et al., 2014) was developed in 2005 by the Solar Energy Research Center (SERC). The system uses the LiCl/H<sub>2</sub>O working pair. The system heat storage capacity was 35 kWh, and the corresponding energy density for short-term storage about 85 kWh/m<sup>3</sup> (Bales, 2008). Its main feature, however, was its ability to operate as a heat pump for cooling or heat production, and the storage function was not the main objective of the system.

Another prototype based on an absorption process using the LiCl/H<sub>2</sub>O couple was constructed (Zhao et al., 2016) at Shanghai Jiao Tong University. The prototype was tested under conditions representative of transition or winter conditions. Although the system was designed for short-term heat storage applications, the working principle could be adapted for long-term purposes (Yu et al., 2014). This process, first presented by (Lourdudoss and Stymme, 1987), is known as the three-phase process. For typical conditions, the stored energy is around 8.5 kWh. Considering a 157-L prototype volume, the system's energy storage density is 54 kWh/m<sup>3</sup>. This value can be increased by 20% by raising the evaporation temperature using a heat recovery technology.

A study was conducted (Liu, 2011) at the LOCIE laboratory at the University Savoie Mont Blanc, using the CaCl<sub>2</sub>/H<sub>2</sub>O couple. Calcium chloride's main advantage is that it is mass produced at very low cost. Although good power levels were obtained in the charging tests, the absorber power during the discharging tests was poor. The reason for this behavior was, according to the authors, due to the presence of noncondensable gases in the system as well as low wettability of the helical fin exchange surfaces where the solution and water film flowed. The absorber power was improved by increasing the evaporator heat transfer fluid (HTF) inlet temperature and mass flow. Therefore, using the system for building space heating applications is possible if technical improvements are made on the prototype.

A closed absorption system involving water and calcium chloride (CaCl<sub>2</sub>) was also proposed by (Quinnell and Davidson, 2012) at the University of Minnesota in the USA. This study was original in that the solution and water tanks were only one stratified reservoir, with low mixing of stored liquids, taking advantage of (1) natural density gradients between the different solutions and (2) the fact that diffusion is 10,000 times slower than thermal conduction. Experimental and simulation studies have been carried out to show the viability of the single-storage-tank design (Quinnell and Davidson, 2012; 2014). The results demonstrated that natural convection does not disrupt the stable mass fraction distribution and therefore that the concept holds promise for long-term storage.

Fumey et al. (2015; 2017) at the EMPA laboratory developed a closed sorption heat storage system based on the NaOH/H<sub>2</sub>O couple. The economic criterion also prevailed in the NaOH salt selection, because its cost is much lower than LiCl or LiBr. The prototype was constructed in a 7-m-long container with solar collectors as a heat source. The system's experimental results in the discharging mode were less than those theoretically calculated. The best measured values were around 1 kW for cases in which a very low temperature difference between the absorber and the evaporator were considered (Daguenet-Frick et al., 2016). Higher temperature differences reduced the absorber power. Problems were encountered in the solution pumping at the absorber/desorber heat exchanger due to cavitation

phenomena generating incomplete tube bundle external surface wetting. The influence of noncondensable gases on the system's performance was also highlighted by the authors.

N'Tsoukpoe et al., (2013) constructed a prototype at the University Savoie Mont Blanc, to test the potential of a long-term absorption heat storage system using the LiBr/H<sub>2</sub>O pair. The prototype was designed to have an 8-kWh heat storage capacity. In general, the charging mode worked in a satisfactory manner with an average generation rate around 2 kW. On the other hand, the results obtained during the discharging tests showed no significant heat transfer between the absorbing falling film and the HTF, even if the absorbing falling film reached a satisfying temperature level. Different reasons were pointed out: the use of copper alloy for the tubes of the absorber/desorber heat exchangers, which did not prove to be corrosion-resistant to the LiBr solution; the presence of noncondensable gases in the reactor; and wettability problems.

Zhang et al. (2014) also designed and constructed an interseasonal absorption thermal energy storage prototype, using the LiBr/H<sub>2</sub>O couple. Experimental results associated with the discharging mode for space heating applications gave heating rates between 12 kW and 7 kW, with the higher values present for a short time at the beginning of the test. The energy storage density of the system associated with the space heating was 110 kWh/m<sup>3</sup>. However, LiBr is an expensive salt, which could limit its extensive use.

In the present study, the innovative KCOOH/H<sub>2</sub>O couple, which to the authors' knowledge has never been used in an absorption heat storage process, was selected and implemented in an absorption heat storage prototype, a first original aspect of the present experiment. As explained in the next section, this couple presents possible advantages in comparison to the other absorption couples presented above. This study also follows several research projects conducted at the University Savoie Mont Blanc in the absorption storage area, as highlighted in the previous section. In this new research stage, an original prototype was developed to overcome the technical difficulties and physical limitations observed on the previous experimental benches. Original heat and mass exchangers and gravitational fluid circulation are also presented. In the following, this absorption heat storage prototype is described and the experimental results obtained are presented and analyzed.

## **2. System description**

### **2.1 Process description**

The operating principle of the long-term solar heat storage process based on the absorption phenomenon is presented in Figure 2. The process is composed of four main components: a desorber, an absorber, a condenser and an evaporator, to which two solution storage tanks (for the diluted and concentrated solution) and an absorbate storage tank are added. The system operates in the charging mode when solar heat is available and in the discharging mode in heating demand periods. In summer, solar heat is received by a flat plate solar thermal collector and is supplied at around 60°C to the diluted solution that is transferred from its storage tank to the desorber. The solution releases the absorbate vapor and becomes concentrated (in absorbent). The absorbate vapor is condensed in the condenser using a heat sink (for example a ground-coupled heat exchanger) and flowed to the absorbate storage tank

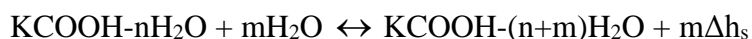
and stored in liquid form. The concentrated solution obtained flows from the desorber into the concentrated solution tank. After this charging period, the storage tanks are disconnected so that there is no mass exchange between the components: energy can therefore be stored in the form of a chemical potential as long as needed. During the following winter or heating period, the discharging phase can occur. The concentrated solution flows to the absorber, where it absorbs the absorbate that is evaporated by the heat transferred from a low-temperature heat source. The heat produced by this exothermic absorption phenomenon can then be used for building heating purposes, at temperatures over 25°C, for example, in a heating floor.

The solution can crystallize in the solution storage tank in this process. Indeed, at the end of the charging process, the mass fraction of absorbent in the solution is high. In the storage tank, the temperature of the hot solution coming from the desorber decreases due to heat loss to the surroundings. Therefore, if the solubility temperature of the solution is reached in the tank, crystals appear. Allowing crystal formation in the tank and thus increasing the solution mass fraction at the end of the charging process can multiply the system's energy storage density several times (N'Tsoukpoe, 2012). Indeed, in the discharging phase, the larger the amount of absorbate available for absorption, the greater the amount of sorption heat that can be recovered. Consequently, during desorption (charging phase), the more absorbate extracted from the diluted solution, the more heat stored. The storage density is then increased by this crystallization and therefore crystallization is relevant for the process's competitiveness, but the technical complexity of the process increases also, in particular pumping and circulating the solution (N'Tsoukpoe, 2013). Therefore, the system's components have to be carefully designed.

## 2.2 KCOOH/H<sub>2</sub>O couple selection

For the absorption storage process, one of the major issues is the choice of the absorbate/absorbent couple. In most of the absorption heat pumps available on the market, two possible couples are used: LiBr/H<sub>2</sub>O or H<sub>2</sub>O/NH<sub>3</sub>. The second choice is usually discarded in the case of storage processes, for security reasons: a large amount of absorbate (in this case NH<sub>3</sub>) has to be stored between the charging and the discharging phases, and NH<sub>3</sub> should be avoided. Water is then the chosen absorbate, although its use imposes strong technical constraints on the system, because it must be operated under low pressure (typically 10–30 mbar, depending on the phase considered and the operating temperatures). As was shown in the literature review presented above, water was the choice of all the tested absorption storage prototypes presented.

The second step is the choice of the absorbent. Four of them have already been tested (LiCl, CaCl<sub>2</sub>, NaOH and LiBr). However, none of them has reached the commercial development stage. In the context of this long-term solar heat storage system, a multicriteria analysis on various possible absorbents (Lefebvre, 2015) has led to the choice of KCOOH for the system. It absorbs water following the equilibrium :



where  $\Delta h_s$  is the sorption heat that is released during the absorption phenomenon.

The H<sub>2</sub>O/KCOOH solution is currently used mainly at low salt concentrations as brine or a biodegradable de-icing solution. It is also widely in use in the oil-drilling industry and as an ice-removing agent for planes (Aittomaki and Lahti, 1997). To the authors' knowledge, it has never been used in an absorption energy storage process. Mixtures of potassium formate and lithium bromide solutions were evaluated in an absorption chiller and showed promising performance (De Lucas et al., 2004). Moreover, potassium formate absorption and desorption characteristics have been tested: Riffat et al. (1996) showed that potassium formate has the potential to be a possible “drop-in” replacement for lithium bromide, because absorption rates of both working fluids were very similar and the heat of absorption only slightly lower when using potassium formate.

The H<sub>2</sub>O/KCOOH solution's thermophysical properties are still not precisely known for concentrations higher than 50% (Lowenstein, 2008; Melinder, 2007). This solution mass fraction range is useful for heat storage process applications. However, data from Balarew et al. (2001), Sidgwick and Gentle (1922), Scatchard and Prentiss (1934), Aittomäki and Lahti (1997), Beyer and Steiger (2010) and Lefebvre (2010) make it possible to draw a Dühring diagram for the KCOOH/H<sub>2</sub>O solution up to a KCOOH mass fraction of 75%, as presented in Figure 3. This couple seems to present equilibrium conditions compatible with the use of solar collectors as a heat source during the summer and with a heating floor as a heat sink during the winter, as presented in Figure 3. Absorption temperatures during the winter phase can produce heat at temperatures between 25 and 36°C (usable by up-to-date heating floors) for KCOOH mass fractions between 62 and 76%, and the corresponding desorption temperatures during the summer are as low as 58°C, which can easily be reached by flat plate solar collectors.

The H<sub>2</sub>O/KCOOH solution is environmentally friendly, nontoxic and nonflammable; has an advantageous theoretical heat storage energy density; and costs less than half the price of the couples usually used in absorption processes (LiBr/H<sub>2</sub>O or LiCl/H<sub>2</sub>O) (Lefebvre, 2015). Its aqueous solution is also weakly alkaline and therefore noncorrosive and biodegradable (Longo and Gasparella, 2016), and has a lower density and viscosity than absorbents such as lithium bromide (Riffat et al., 1998). These advantages together with its relatively low cost make it a prime choice as the absorbent for the heat storage process.

### **3. Prototype description**

#### **3.1 Prototype components and dimensioning**

A prototype was developed to demonstrate the feasibility of storing solar heat efficiently using this KCOOH/H<sub>2</sub>O absorption process. It was designed to store about 8 kWh of heat and to produce a heating power of approximately 1 kW.

In this storage process, the charging and discharging phases are successive, allowing the absorption and desorption phenomena to take place in the same component, as well as evaporation and condensation. For heat exchangers, a sandwich grooved vertical plate configuration was then chosen (Figure 4(b)). As mentioned by (Do et al., 2008) and (Guo et al., 2011), a grooved surface allows better wetting of the falling films flowing along and within the grooves, which can ensure uniform distribution and wetting over the entire

exchange surfaces. The plates are 50 cm high and 40 cm wide. Both exchangers are located in the same reactor, situated above the storage tank (Figure 4(a)) to allow the flows to return to these tanks by gravity.

A double-envelope configuration was chosen for the solution tank, where the 70-L internal cylinder (in glass) contains the KCOOH solution, and the annulus between the internal and external cylinders (in acrylic glass) contains water as the heat transfer fluid to control the tank's temperature. Only one solution tank is used, such that the solution mass fraction changes progressively over the charging and discharging phases. The prototype was designed to be able to test the solution's crystallization functionality. Thus, the solution is pumped out of the top of the solution tank using a float, and it flows back to the bottom of the tank. This avoids pumping crystals from the solution tank, as the crystals' density is higher than the solution's density. A double envelope was also designed to control the temperature of the stainless-steel 55-L water storage tank.

The picture and the scheme of this prototype are presented in Figures 5 and 6, respectively. Three thermal modules are used in the prototype (external heaters/coolers in Figure 5). They control the solution tank temperature, the absorber/desorber heat transfer fluid temperature, and the water tank and the evaporator/condenser heat transfer fluid temperatures, respectively. W1 and W2 (Figure 6) are magnetic-driven volumetric pumps.

The capability of the reactor, the solution tank and the water tank to maintain vacuum conditions was tested prior to the experimental tests. The maximum leakage rate measured was  $2.67 \cdot 10^{-4}$  (mbar.l)/s, which is satisfactory for this type of experiment. Consequently, a vacuum pump was used (W7 in Figure 6) to put the reactor container, solution tank and water tank in vacuum conditions before the experimental tests began, but the vacuum pump was off during the tests.

### **3.2 Instrumentation**

The prototype was strongly instrumented for analysis of the functioning of this process (temperature, pressure, mass flow, volumetric flow, density, levels of the internal and external fluids were all measured). Probe positions are illustrated in Figure 6. The types and precision of the measurements are presented in Table 1.

### **3.3 Experimental conditions**

Experiments were carried out in the conditions representing the system's functioning in the case of interseasonal solar heat storage for building heating in a French climate. The temperature of the desorber HTF should represent the temperature of the solar collectors during the summer. To ensure the highest possible solar collector efficiency, the temperature should be as low as possible, so the process was tested at desorber temperatures between 50 and 70°C. The corresponding condenser temperature should represent a heat release to an external heat sink. This sink could be the ambient air or a geothermal pipe, for example, so the process was tested for a condenser HTF entering at a temperature of 15°C. During the discharging phase, the HTF of the evaporator should represent the temperature of an external heat source during the winter period. Again, this source could be the ambient air or a geothermal pipe, so the process was tested for an evaporator HTF entering at a temperature of

15°C, assuming a constant ground temperature over the year. The corresponding absorber should provide heat for building heating. For this type of absorption process, similarly to the conventional heat pumps, the lower the absorber temperature, the higher the system performance. Thus, this process was assumed to be connected with a low-temperature heat floor in an efficient building; the absorber HTF temperature was then tested between 20 and 30°C.

The external fluid mass flows were chosen both sufficiently high to ensure both turbulence for an acceptable heat transfer rate in the exchangers, and sufficiently low for an acceptable temperature difference between the inlet and the outlet of the fluids to allow measurable heat flux in these components. The solution and the internal water flows over the grooved plates were optimized, as a compromise between different constraints:

- The mass flow should be low enough for a measurable mass fraction difference between the solution inlet and outlet of the desorber/absorber or a measurable mass flow difference between the inlet and outlet of the evaporator.
- It should also be low enough to have a thin film over the plates and consequently efficient heating or cooling of the film interface by the external HTF.
- However, it should be high enough to correctly wet the exchanger plates.
- It was also linked to technical constraints of the prototype: at excessively high mass flow rates, the solution overflowed the exchanger outlet funnel.

The tests were conducted to prove the feasibility of absorption storage using the KCOOH/H<sub>2</sub>O couple. Thus, tests were performed in stable conditions (except for the solution mass fraction, which changes through the absorption and desorption processes). The test lengths were limited due to laboratory security constraints (the system could not be left to function without someone in the room to check the machine). The values of the experimental conditions tested are presented in Tables 2 and 3.

## 4. Experimental results

### 4.1 Charging tests

An example of charging test results is presented in Figure 7. The detailed test conditions are shown in Table 2, in the first column (June 23<sup>rd</sup>). During this 1.5-h test, the external parameters were kept constant. During the first hour of the test (before 10:00, Figure 7(a)), the internal parameters were also nearly constant. The temperature of the HTF decreased in the reactor (TK12 and TK14), providing heat to the solution for the desorption process. The heat provided to the desorber was about 2 kW during that period (Figure 7(b)). At the same time, the condenser HTF temperature increased in the reactor (TK2 and TK13), as the desorbed water from the solution condensed on the cooled condenser walls. The corresponding condensation heat was about 1.5 kW during that period (Figure 7(b): a negative value as the heat is extracted from the process). The sorption enthalpy is usually about 15% larger than the phase change enthalpy of water. The 500-W difference between the two heats involved is explained by the difference between the phenomena and by possible heat losses to the surroundings in the reactor: the reactor is not insulated and despite the low convective heat

losses due to the low pressure in the system, radiative and conductive heat transfers in the connecting pipes and mechanical stands could transfer heat to the surroundings. During this first period, the temperature of the solution exiting the reactor was around 50°C (TK9 in Figure 7(a)). This sensible heat is later lost to the surroundings in the solution storage tank. However, a heat exchanger between the entering and exiting solution of the reactor is not a solution during that charging phase: when the hot solution at a high mass fraction of KCOOH exits the reactor, sudden cooling could lead to crystal formation in the heat exchanger, meaning the clogging of the exchanger.

After the first hour (after 10:00, Figure 7(a)), the temperature of the solution entering the reactor increased progressively. Indeed, the flow in the solution tank is of the plug-flow type, and the external cooling of the solution tank did not manage to keep the solution temperature constant at 23°C during the whole test. This temperature increase led to the small decrease of the absorbed heat in the desorber during the last half hour of the test (Figure 7(b)).

Other experimental results obtained during charging tests are presented in Table 2. Important criteria to weigh the performance of the system are the rate of desorbed water and the power exchanged at the desorber, i.e., the power that would be supplied by the solar collectors in a solar storage system. The rate of desorbed water increased when:

- The flow of solution increased within the range tested. For example, comparing the test of June 30<sup>th</sup> with the test conducted on June 23<sup>rd</sup>, the solution flow rate increased from 51 kg/h to 60 kg/h. This increase resulted in a moderate 5% increase of the desorbed water flow rate. This result was confirmed by the July 5<sup>th</sup> test, when a low flow rate of 40 kg/h was tested, decreasing the rate of desorbed water by more than 30%. Increasing the flow rate of the solution improved the efficiency of the exchangers because their wetting rate was increased. This result is only valid for the range of flow rates studied (40–60 kg/h). Indeed, there exists an optimal solution flow rate beyond which a flow rate increase decreases the performance of the process, since the heat transfer from the exchanger wall to the liquid/vapor interface decreases with the thickness of the film (Huaylla et al., 2015).
- The desorption temperature increased. Indeed, comparing the June 23<sup>rd</sup> test with the July 4<sup>th</sup> test, the HTF temperature of the desorber increased from 57°C to 64°C, improving the rate of desorbed water by 7%. For the LiBr/H<sub>2</sub>O couple, N'Tsoukpoe et al. (N'Tsoukpoe et al., 2012) showed theoretically that a minimum desorption temperature must be chosen for this storage process. Below this minimum value, the water is not desorbed from the solution but only a sensible heat transfer is observed. This was also experimentally observed for the KCOOH-H<sub>2</sub>O couple on the July 12<sup>th</sup> test, when a desorber temperature of 49°C divided the rate of water desorption by a factor of 3 compared to a temperature of 57°C. However, during the desorption tests conducted, the HTF temperature of the desorber could not be increased to temperatures higher than 70°C; otherwise boiling of the solution was observed on the heat exchanger plates, leading to droplet ejections from the film and thus a decrease in desorber performance.
- The mass fraction of the solution decreased. At high mass fractions, the driving force of the desorption process (linked to the difference between the equilibrium pressure of the solution interface and the actual pressure of the water vapor in the reactor) decreased, and therefore the rate of desorbed water decreased. The test conducted on July 20<sup>th</sup> and 21<sup>st</sup> desorbed an

average of 1.13 kg/h and 1.05 kg/h of water, respectively, about 30% less than the 1.51 kg/h and 1.61 kg/h rate obtained on June 23<sup>rd</sup> and July 4<sup>th</sup> in similar conditions, but at lower mass fractions.

#### 4.2 Discharging tests

An example of a charging test result is presented in Figure 8. The detailed test conditions are shown in Table 3, in the second column (July 1<sup>st</sup>). During this test, the air temperature in the room was between 29 and 32°C. Consequently, the absorber HTF temperature fluctuated slightly, due to the functioning of the thermal module heat pump (Figure 8(a)) that had to regulate the HTF temperature close to the ambient temperature. However, this fluctuation was limited to a  $\pm 0.5^\circ\text{C}$  around 26°C. The HTF crossing the absorber was heated by the absorption phenomenon occurring in the solution. Moreover, the temperature pinch between the HTF and the solution was very low in this heat exchanger, lower than 2°C. The corresponding heat flux provided to the HTF was around 500 W (Figure 8(b)) throughout the test. During the same period, the HTF crossing the evaporator only provided about 130 W to the internal water for evaporation. The discrepancy cannot be explained by the difference between the phase change enthalpy and the sorption enthalpy. In this case again, heat gains from the surroundings provided heat to the reactor for the water evaporation: indeed, the evaporator temperature was set at 15°C to represent winter conditions, but the tests were conducted in a room at about 30°C, and therefore the external walls of the system could contribute to water evaporation.

Other experimental results obtained during discharging tests are presented in Table 3. For the absorption tests, the main target is the heating of the absorber HTF. The power delivered by the absorber to its HTF increased when:

- The solution flow rate increased. For tests taking place on June 27<sup>th</sup> (solution average flow rate of 96 kg/h), July 7<sup>th</sup> (69 kg/h) and July 13<sup>th</sup> (38 kg/h), the average power outputs were 429 W, 309 W and 245 W, respectively. These results show the importance of the solution's flow rate, because cutting it in half also resulted in a twofold decrease of the power released. Funnels located at the bottom of the heat exchanger plates receive the falling films before the flows exit the reactor. Due to overflowing of the solution funnel at high flow rates, it was not possible to reach solution mass flows higher than 100 kg/h on this heat exchanger, but it is likely that a further increase of the solution flow rate would still lead to an increase in the heat provided because the wetting rates observed on the absorber plates were generally low in the conditions tested.
- The water flow rate on the evaporator plates increased. Comparing the test of July 11<sup>th</sup> with the test conducted on June 27<sup>th</sup>, the water flow rate decreased from 103 kg/h to 64 kg/h, decreasing the heat release from 430 W to 340 W. However, this parameter had a smaller impact than the solution mass flow.
- The absorber temperature decreased, as expected. For tests taking place on July 12<sup>th</sup>, June 27<sup>th</sup> and July 22<sup>nd</sup>, the temperature HTF entering the reactor was 20°C, 25°C and 30°C, respectively. The average heating power outputs were then equal to 660, 430 W and 400 W, respectively, even though the mass fraction of the solution was higher during the latter test than for the previous one. This strong dependence on the absorber temperature eliminated the use of this couple in a heat storage process at high temperatures. It is therefore limited to heating floor diffusers.

The influence of the HTF mass flow rate in the evaporator was negligible within the range tested (300–400 kg/h). For higher mass fractions, it was expected that the heat produced would be greater than at lower mass fractions, but the tests did not show that this parameter had a strong influence. The results obtained on June 27<sup>th</sup> and July 20<sup>th</sup> were similar, although the mass fraction was much higher during the second test than the first one.

In our prototype, crystals appeared in the solution tank only at very high mass fractions, above 73%. This mass fraction, compared to the temperature of the tank during that period, does not correspond to the theoretical saturation values expected. Further tests seem to be needed to determine the precise saturation line of the KCOOH aqueous solution.

### **4.3 General conclusions on the experimental results**

The heat storage process with the KCOOH/H<sub>2</sub>O couple was proven by this experiment. Desorption tests showed the possible charge of this storage system at temperatures as low as 50–60°C, which can easily be reached by flat plate solar collectors. Discharge tests demonstrated heat production at a sufficient temperature level for building heating purposes using a heating floor (>25°C), with a solution at the absorber outlet at temperatures higher than 30°C. Absorption powers of about 400 W were often obtained in the tested conditions, and for the best conditions, average power of 660 W was provided by the absorber and transferred to the heat transfer fluid. Moreover, crystallization was reached in the solution storage tank (July 21<sup>st</sup> and 22<sup>nd</sup>). The following dilution of the crystals during the absorption process was possible (July 22<sup>nd</sup> test, Table 3). This shows that the system can be charged and discharged.

These tests were not conducted with the objective of weighing the storage density of the process, given that they were only feasibility demonstration tests. Consequently, the tests were only performed over short periods (about 1–4 h), and the whole mass fraction range of the solution was not exploited over any test (concentrations lower than 60% were not tested, for example, but theoretically this could be an option, as shown in Figure 4). It is therefore not possible to calculate the storage density using this couple: further tests with an improved prototype would be necessary.

Indeed, the absorption power obtained was limited, due to problems wetting the falling film exchangers, both for the solution on the absorber/desorber and the water on the evaporator. This low wettability stems from the low flow rates that are used in this storage process for a higher process efficiency, in contrast to the recirculation rates that are usually accepted in absorption chillers (Huaylla et al., 2015). Further investigation is needed to develop efficient falling film exchangers for this specific application. Moreover, the sensitivity of the process functioning to the desorber temperature was observed: at high desorption temperatures (in this case above 75°C), the solution boiled on the plates, leading to droplets of solution ejected from the film. This phenomenon has to be taken into account during the desorber design phase. An option would be to stack several plates in parallel, such that the ejected droplets from one plate could be received by the facing plate. However, stacks combining condenser and desorber plates facing each other, which could have been chosen for compactness of the reactor and to decrease the vapor pressure drop between these components has to be discarded, to avoid mixing risks between the solution and water flows.

## 5. Conclusion and outlooks

This study has proved that the KCOOH/H<sub>2</sub>O couple can be used in absorption processes. The performance of this couple is somewhat lower than that obtained by the LiBr/H<sub>2</sub>O couple. This confirms the choice of the former in the case of heat pumps, for example, for which the amount of absorbent is limited. However, in the storage process, the choice of this innovative couple could be an option, because it substantially decreases the investment cost of the process. Another major advantage of this sorbent is its low corrosivity, compared to the reference sorbent. However, the use of this innovative couple would be limited to building heating at low temperatures (lower than 30°C) and may not contribute to domestic hot water production, for example. Further work is still needed on the characterization of the couple: parameters such as the enthalpy of the solution as a function of its temperature and mass fraction as well as the diffusion coefficient of water into KCOOH solutions could not be found in the literature in the mass fraction range required for this storage process. This characterization work is still needed to model and optimize the system.

## References

- Aittomiiki A. and A. Lahti, Potassium formate as a secondary refrigerant, *Int J. Refrig.* 20 (4), p. 276-282 (1997).
- Balarew C., Dirkse T., Golubchikov O.A., Salomon M., IUPAC-NIST Solubility Data Series. 73. Metal and Ammonium Formate Systems, *Journal of Physical and Chemical Reference Data* 30 (1), p. 9-14 (2001)
- Bales C., Nordlander S.; TCA Evaluation - Lab measurements, modelling and system simulation. Report of the Solar Research Energy Center (SERC), Sweden; p. 2–22 (2005).
- Bales C., Laboratory Tests of Chemical Reactions and Prototype Sorption Storage Units. Report of IEA Solar Heating and Cooling programme – Task 32: Advanced storage concepts for solar and low energy buildings, p. 3–8 (2008).
- Beyer R., Steiger M., Vapor Pressure Measurements of NaHCOO + H<sub>2</sub>O and KHCOO + H<sub>2</sub>O from 278 to 308 K and Representation with an Ion Interaction (Pitzer) Model, *J. Chem. Eng. Data* 55, p. 830–838 (2010).
- Daguenet-Frick X., Gantenbein P., Müller J., Fumey B., Weber R.; Seasonal thermochemical energy storage: Comparison of the experimental results with the modelling of the falling film tube bundle heat and mass exchanger unit. *Renew. Energ.* 110, p. 1-12 (2016).
- De Lucas A., Donate M., Molero C., Villasenor J., Rodriguez J.F., Performance evaluation and simulation of a new absorbent for an absorption refrigeration system, *International Journal of Refrigeration* 27, p. 324–330 (2004).
- Do K.H., S.J. Kim, S.V. Garimella, A mathematical model for analyzing the thermal characteristics of a flat micro heat pipe with a grooved wick, *Int. J. Heat Mass Tran.* 51, p. 4637-4650 (2008).
- Fumey B., Weber R., Gantenbein P., Daguenet-Frick X., Stoller S., Fricker R., Dorer V.; Operation results of a closed sorption heat storage prototype. *Energy Procedia* 73, p. 324-330 (2015).

- Fumey B., Weber R., Baldini L., Liquid sorption heat storage – A proof of concept based on lab measurements with a novel spiral fined heat and mass exchanger design, *Appl. Energy* 200, p. 215-225 (2017)
- Guo L., Z.C. Liu, Y. Yan, Z.W. Han, Numerical modeling and analysis of grooved surface applied to film cooling. *J. Bionic Eng.* 8, p. 464-473 (2011).
- Hadorn J.-C., Advanced storage concepts for active solar energy, IEA-SHC Task 32 2003-2007, Eurosun 2008 (1<sup>st</sup> international congress on Heating, Cooling and Buildings), Lisbon (Portugal), 7<sup>th</sup> -10<sup>th</sup> October 2008.
- Huaylla F., N. Le Pierrès, B. Stutz, Numerical and experimental analysis of an absorption reactor using LiBr/H<sub>2</sub>O for solar heat long-term storage, ECCE10 (10th European Congress of Chemical Engineering), Nice (France), 27<sup>th</sup> september-1<sup>st</sup> october 2015.
- Ibrahim N.I., Al-Sulaiman F.A., Nasir Ani F., Solar absorption systems with integrated absorption energy storage—A review, *Renewable and Sustainable Energy Reviews*, In press, Available online 8 July 2017
- IEA, Energy efficiency market report 2015, International Energy Agency, OECD/IEA (2015).
- Lefebvre E., Procédé par absorption avec stockage d'énergie solaire intersaisonnier intensifié par la cristallisation de l'absorbant : Recherche & caractérisation thermodynamique de nouveaux couples; Conception de la cuve de stockage, PhD thesis of Lyon 1 University (in French) (2015).
- Liu H.; Inter-seasonal solar energy storage for buildings by absorption, PhD thesis of the University of Grenoble, France (2011).
- Longo G.A. ,A. Gasparella, Experimental measurement of thermophysical properties of H<sub>2</sub>O/KCOOH (potassium formate) desiccant, *Int. J. of Refr.* 62, p. 106–113 (2016).
- Lourdudoss S., Stymme H.; Energy storing absorption heat pump process. *Int. J. Energ. Res.* 11, p. 263–274 (1987).
- N'Tsoukpoe K.E., Liu H., Le Pierrès N., Luo L.; A review on long-term sorption solar energy storage. *Renew. Sust. Energ. Rev.* 13, p. 2385-2396 (2009).
- N'Tsoukpoe KE, N. Le Pierrès, L. Luo, Numerical dynamic simulation and analysis of a lithium bromide/water long term solar heat storage system. *Energy* 37 (1), p. 346-358 (2012).
- N'Tsoukpoe K. E., N. Le Pierrès, L. Luo, Experimentation of a LiBr–H<sub>2</sub>O absorption heat storage process: prototype design and first results, *Energy* 53, p. 179-198 (2013).
- Quinnell J. A., Davidson J.H.; Mass transfer during sensible charging of a hybrid absorption/sensible storage tank. *Energy Procedia* 30, p. 353–361 (2012).
- Quinnell J. A., Davidson J.H.; Heat and mass transfer during heating of a hybrid absorption/sensible storage tank. *Solar Energy* 104, p. 19–28, (2014).
- Riffat S.B., James S.E., Wong C.W., Experimental analysis of the absorption and desorption rates of HCOOK/H<sub>2</sub>O and LiBr/H<sub>2</sub>O, *Int. J. Energy Res.*, 22, p. 1099-1103 (1998)
- Scatchard G., Prentiss S.S., The Freezing Points of Aqueous Solutions. VI. Potassium, Sodium and Lithium Formates and Acetates, *J. Am. Chem. Soc.*, 56 (4), p 807–811 (1934).
- Sidgwick N.V. and Gentle J.A., CCXXI.-The solubilities of the alkali formates and acetates in water, *J of the Chem. Soc. Trans*, 121, p.1837-1843 (1922).
- Wokon M., Kohzer A., Linder M., Investigations on thermochemical energy storage based on technical grade manganese-iron oxide in a lab-scale packed bed reactor, *Solar Energy* 153 (1), p. 200-214 (2017). Yu N., Wang R. Z., Lu Z. S., Wang L. W., Ishugah T.F.; Evaluation of a three-phase sorption cycle for thermal energy storage. *Energy* 67, p. 468-478 (2014).

Zhang X., M. Li, W. Shi, B. Wang, X. Li, Experimental investigation on charging and discharging performance of absorption thermal energy storage system, *En. Conv. and Manag.* 85, p.425–434 (2014).

Zhang H., Baeyens J., Cáceres G., Degève J., Lv Y., Thermal energy storage: Recent developments and practical aspects, *Prog. in Energy and Comb. Sc.* 53, p. 1-40 (2016). Zhao Y. J., Wang R. Z., Li T. X., Nomura Y.; Investigation of a 10 kWh sorption heat storage device for effective utilization of low-grade thermal energy. *Energy* 113, p. 739–747 (2016).

### **Acknowledgements**

This work has been financed by the ANR (French National Research Agency) under the research project PROSSIS2 ANR-2011-SEED-0011-01.

Table 1. Technical characteristics of the system sensors ('Name' refers to Figure 6)

	Name	Precision
Coriolis Flowmeter	F1 and F2	<i>Mass flow:</i> If mass flow < 190 kg/h, 0.19 kg/h. If mass flow $\geq$ 190 kg/h, 0.1% of the measured value. <i>Density:</i> 1 kg/m <sup>3</sup> .
Coriolis Flowmeter	F3	<i>Mass flow:</i> 0.15% of the measured value + zero stability <i>Density:</i> 2 kg/m <sup>3</sup>
Coriolis Flowmeter	F4 and F5	<i>Mass flow:</i> 0.1% of the measured value + zero stability <i>Density:</i> 1 kg/m <sup>3</sup> .
Rotameter	F6	1% of the measured value
Rotameter	F7	Uncertainty: 4% of full scale (max: 500 kg/h)
Temperature sensors	TK, TT	0.2 °C
Pressure sensor	P1	0,25 mbar
Pressure sensor	P2	0.5% of reading
Pressure sensor	P3 and P4	0.3 mbar
Level sensors	L1 and L2	1.5% of probe length

Table 2. Experimental results of the charging tests.

Date	23/6/16	30/6/16	4/7/16	5/7/16	7/7/16	11/7/16	11/7/16	12/7/16	19/7/16	20/7/16	21/7/16
length	1h31	2h00	1h51	1h24	1h44	1h36	1h18	1h30	2h15	1h07	2h15
Condenser HTF mass flow [kg/h]	300										
Desorber HTF mass flow [kg/h]	300				400	300					
Solution mass flow [kg/h]	50,9	61	48,2	40,8	55,6	40	51	47,4	45	65	57
Desorber HTF inlet temperature [°C]	57,5	57	64	56,5	60,2	68	68	49,4	65,6	66	66
Condenser HTF inlet temperature [°C]	15										
initial mass fraction in the solution tank [%m]	72,1	71,6	73,3	75,2	73,5	74,2	74,6	73,5	75,3	77,6	77,5
Final mass fraction in the solution tank [%m]	74	75,3	76,7	77,3	77	76,7	77,2	74,6	77,7	79,4	80,5
average mass fraction variation [%/h]	1,25	1,95	1,78	1,34	2,08	1,63	2,00	0,80	1,07	1,64	1,33
Desorber heat [kW]	1,81	2,05	2,06	1,44	2,01	1,72	1,92	1,05	1,77	1,6	1,52
Condenser heat [kW]	-1,52	-1,65	-1,64	-1,22	-1,66	-1,54	-1,63	-0,82	-1,53	-1,29	-1,08
Crystals in the solution tank	No	No	No	No	No	No	No	No	No	No	Yes
Desorbed water flow rate [kg/h]	1,51	1,57	1,61	1,05	1,51	1,35	1,47	0,61	1,33	1,13	1,05

Table 3. Experimental results of the discharging tests.

Date	27/6/16	1/7/16	4/7/16	7/7/16	8/7/16	11/7/16	12/7/16	13/7/16	19/7/16	20/7/16	21/7/16	22/7/16
length	1h53	2h57	3h19	2h40	4h00	3h00	3h18	3h41	2h56	2h46	2h46	1h28
Evaporator HTF mass flow [kg/h]	300		400			300						
Absorber HTF mass flow [kg/h]	300											
Solution mass flow [kg/h]	95,8	98,7	98,6	69	70,6	97,1	96,3	38,4	93,8	89,9	52,8	93,8
Water mass flow [kg/h]	103,6	92,5	102,1	94,3	115,9	64,2	108,6	107,9	98,7	102	105,4	100,3
Absorber HTF inlet temperature [°C]	25		30	25			20	25				30
Evaporator HTF inlet temperature [°C]	15											
initial mass fraction in the solution tank [%m]	72,9	74,72	75,9	73,9	76,2	75,9	76,6	74,4	75	77,8	79,2	75,2
Final mass fraction in the solution tank [%m]	70,3	71,1	73,2	72	72,6	73,7	73,2	72,4	73,4	75,6	76,6	73,7
average mass fraction variation [%/h]	2,64	3,59	2,66	1,83	3,67	2,17	3,38	1,98	1,59	2,25	2,65	1,50
Absorber heat [W]	-429	-496	-190	-309	-367	-337	-661	-245	-223	-398	-401	-404
Evaporator heat [W]	114	136	184	144	138	91	128	162	159	169	180	150
Crystals in the solution tank	No	No	No	No	No	No	No	No	No	No	No	Yes

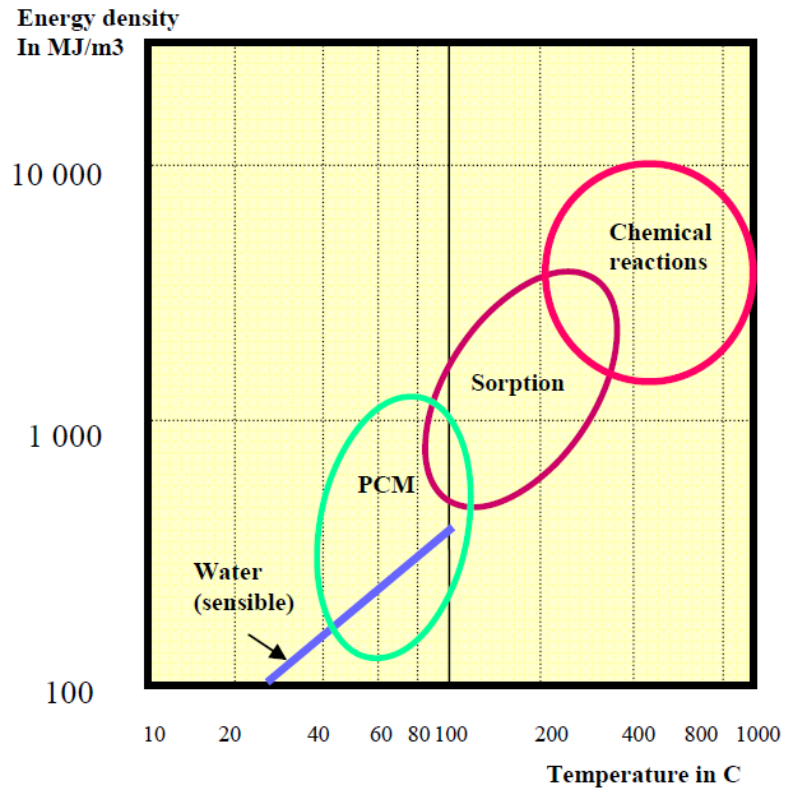
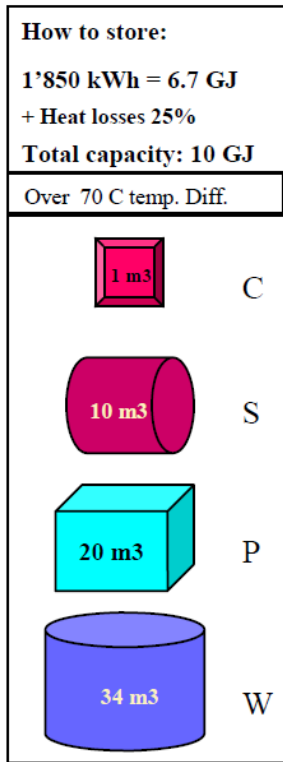


Figure 1: Energy density of energy storage methods (Hadorn, 2008)

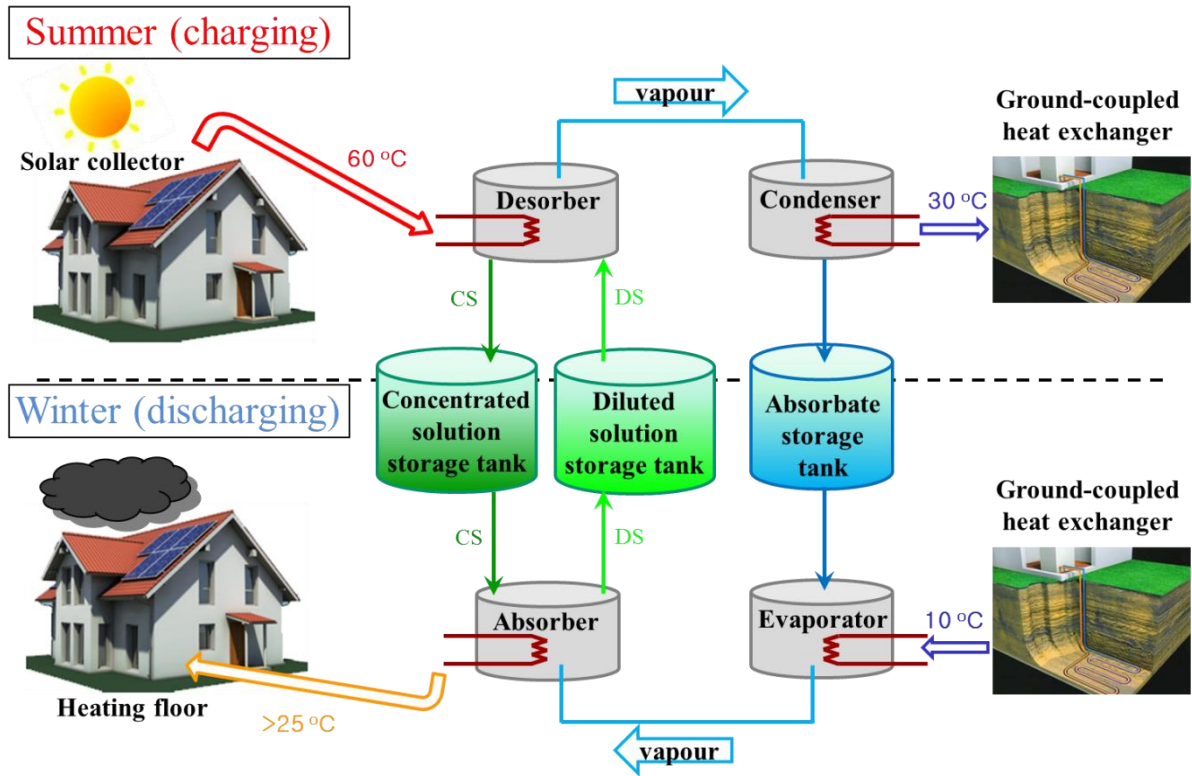


Figure 2. Absorption storage system principle (CS: concentrated solution; DS: diluted solution) (N'Tsoukpoe et al., 2013)

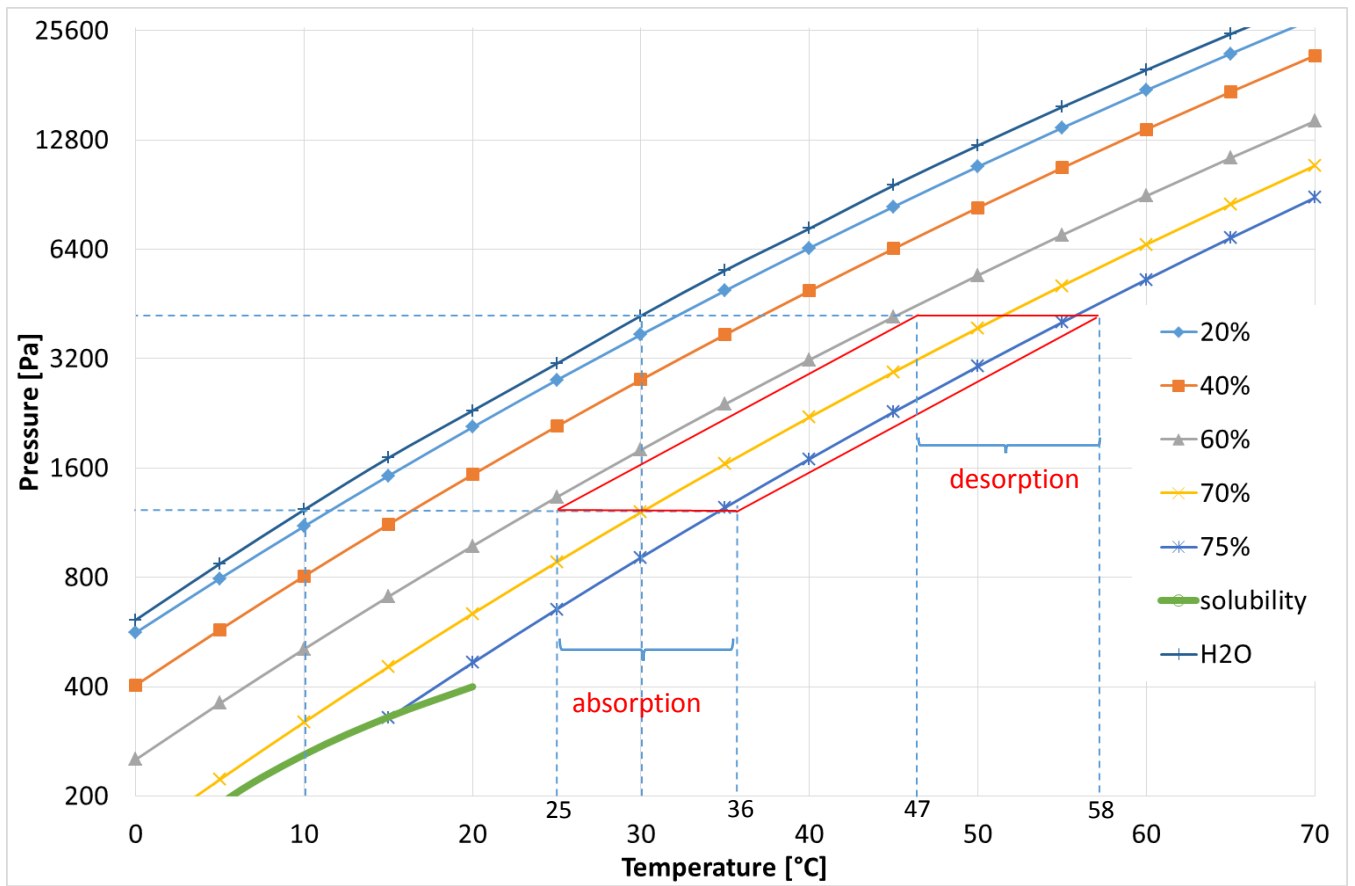


Figure 3: Dühring diagram for the KCOOH-H<sub>2</sub>O solution and operating conditions of the storage cycle

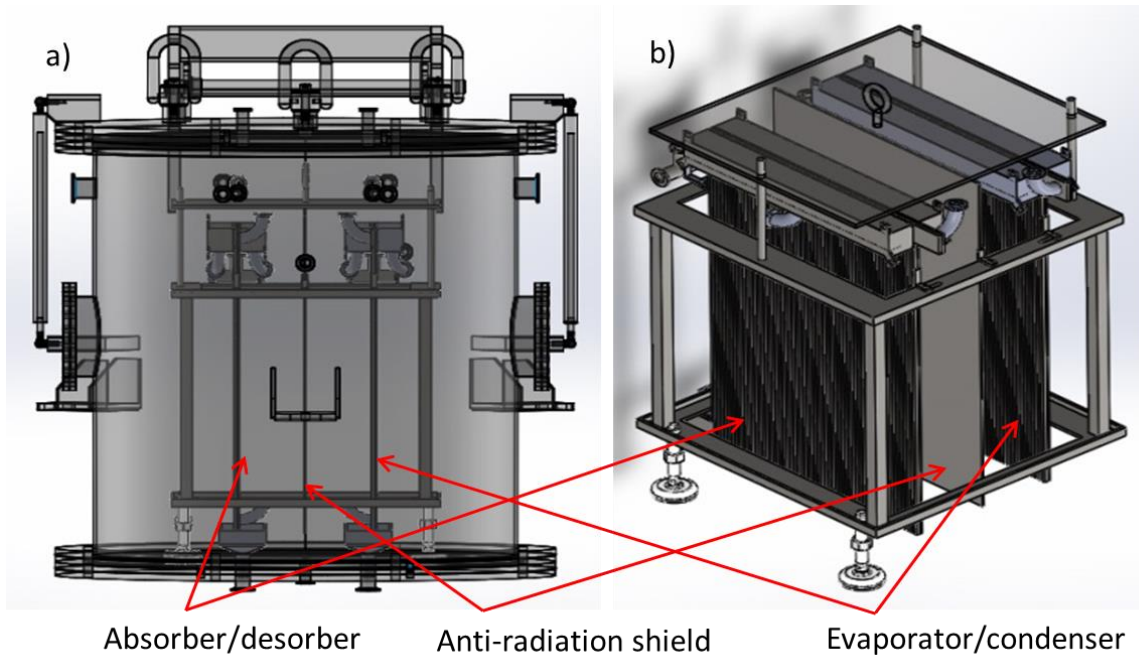


Figure 4. (a) Scheme of the reactor, (b) 3D-view of the heat and mass exchangers in the reactor

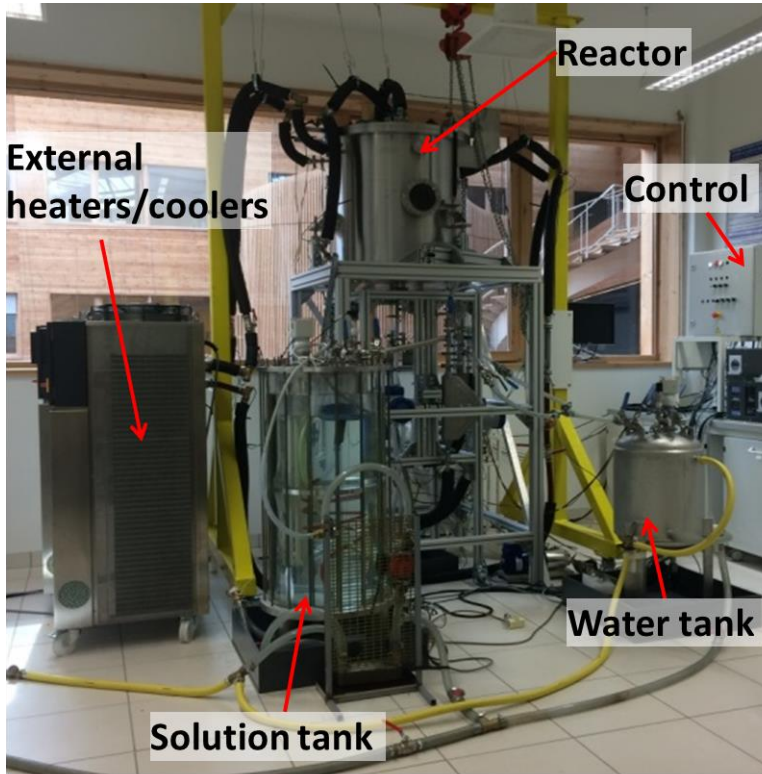


Figure 5. Picture of the prototype

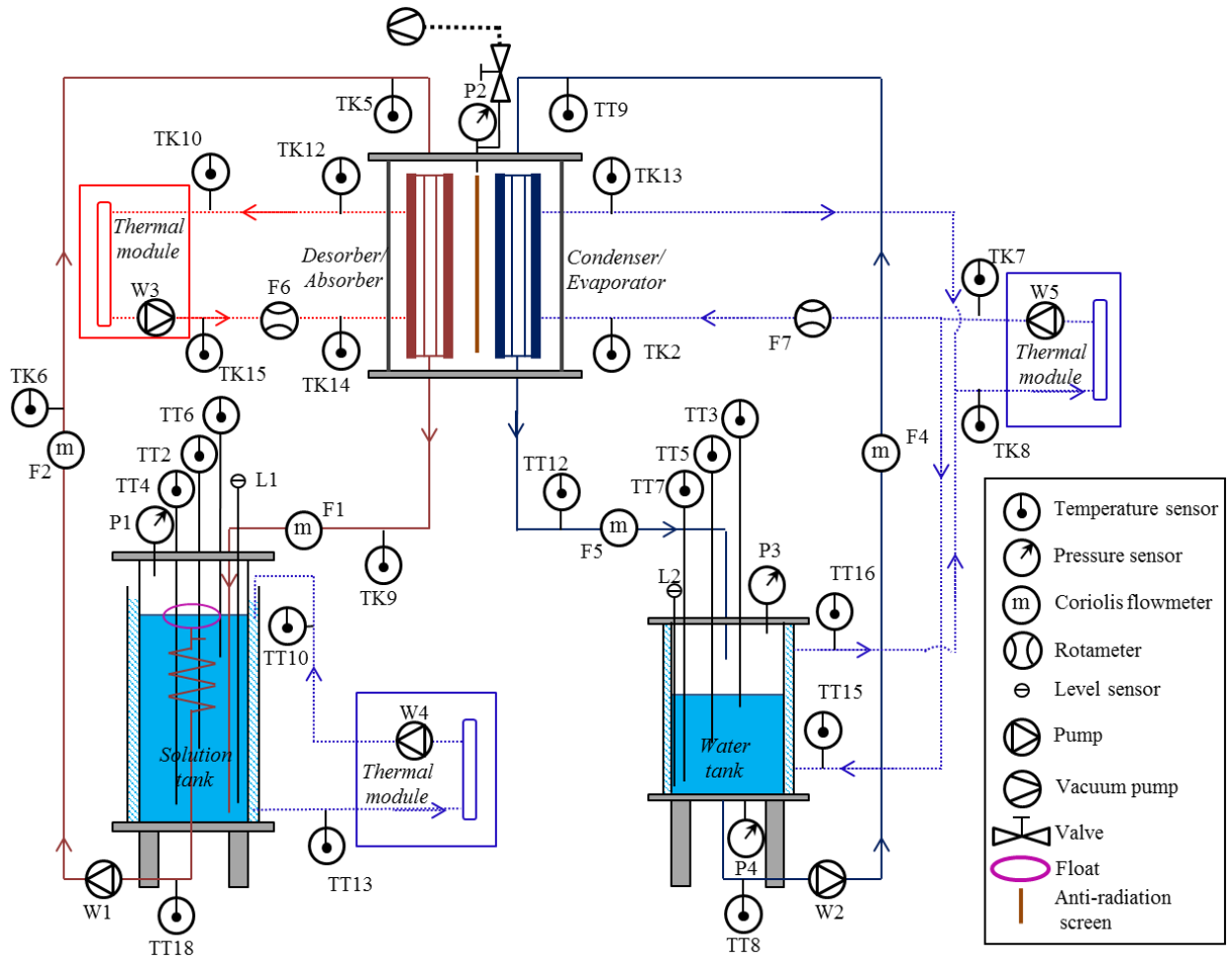


Figure 6: Prototype instrumentation

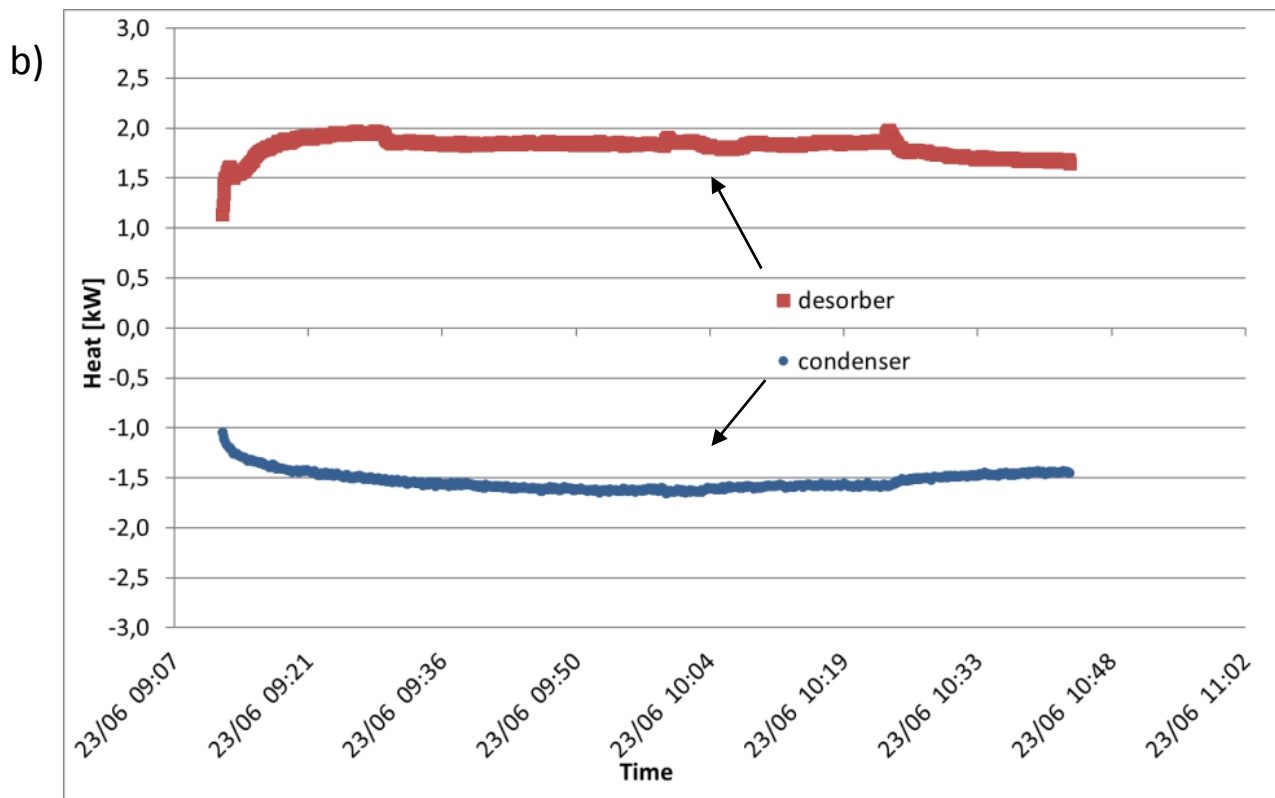
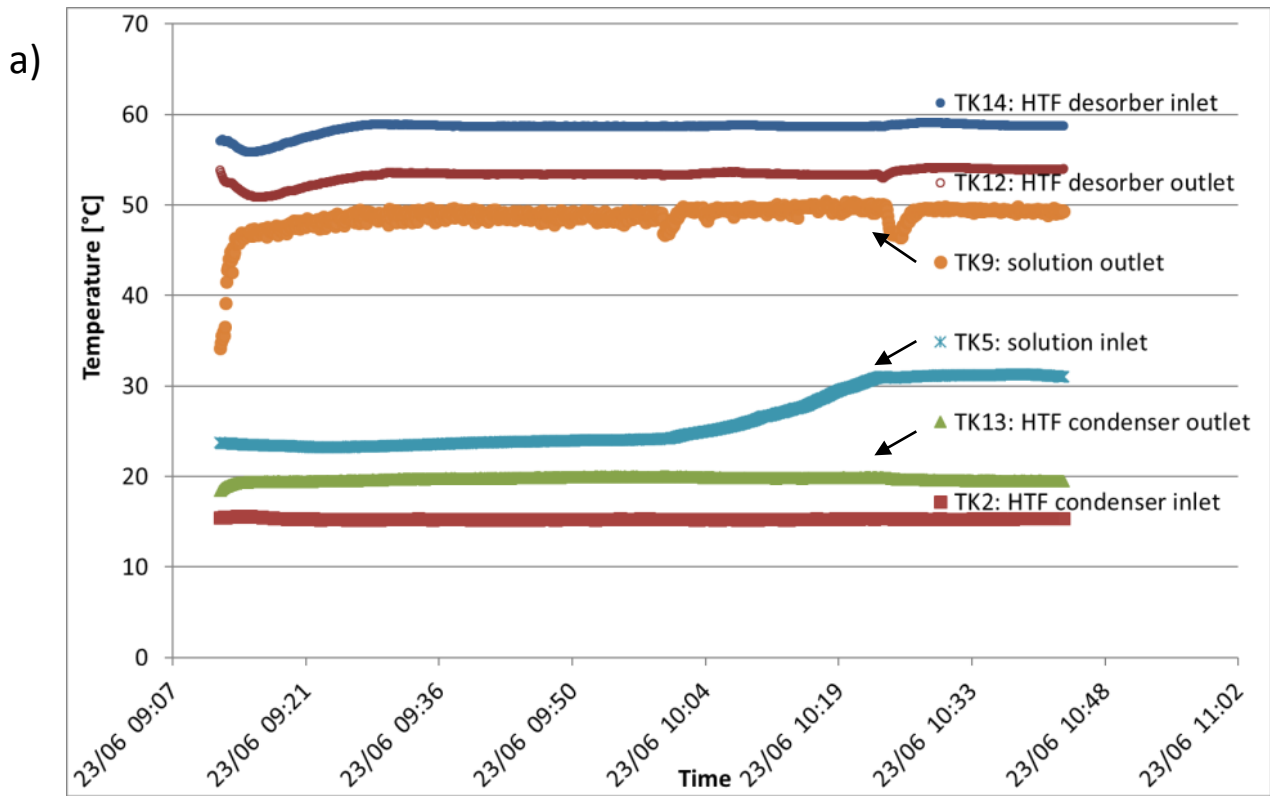


Figure 7. Charging test of June 23<sup>rd</sup>, 2016: temperatures in the components (a) and corresponding heat powers (b).

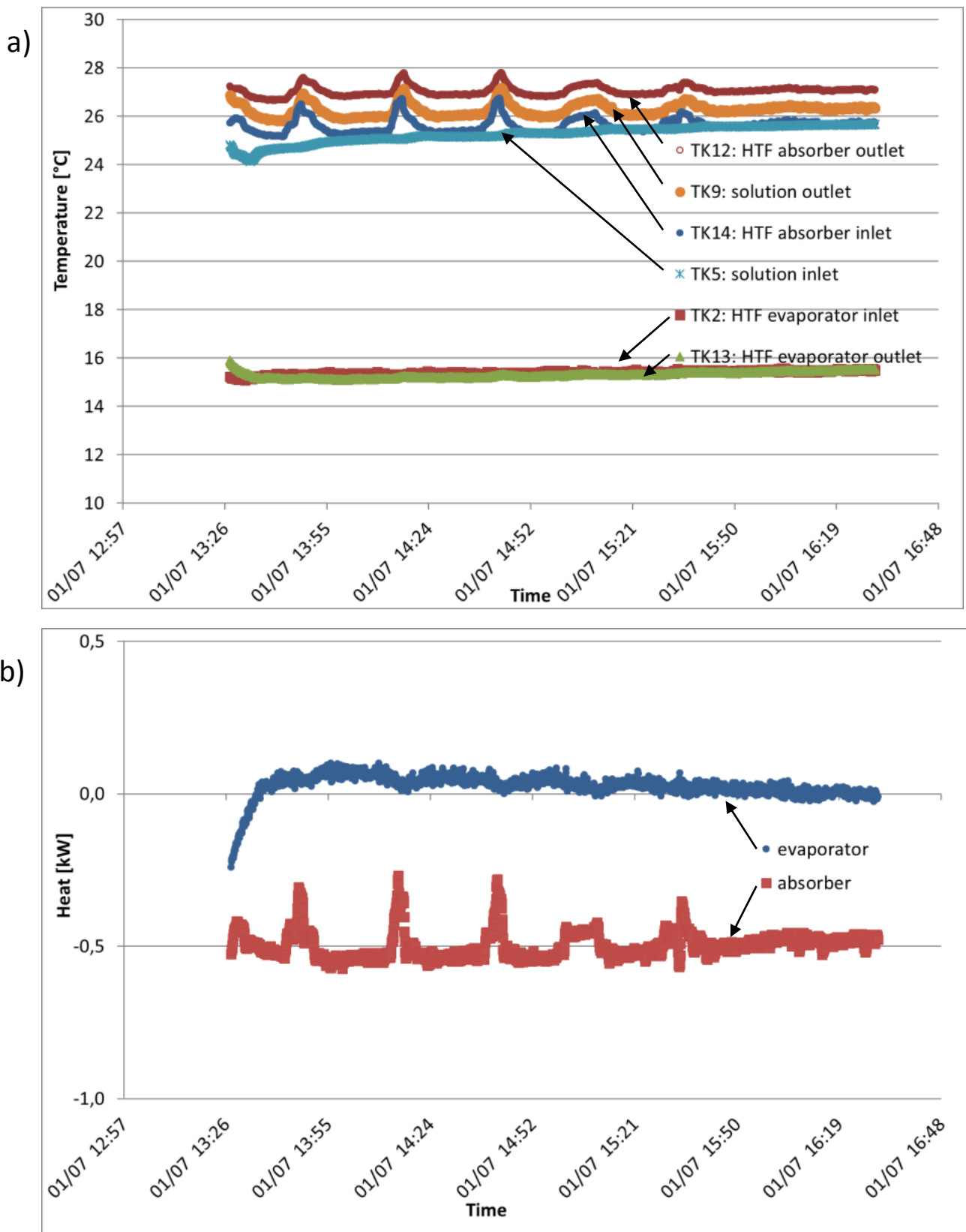


Figure 8: Charging test taking place on July 1<sup>st</sup>, 2016: temperatures in the components (a) and corresponding heat powers (b)